Analysis of Boron Arsenide (BAs) Band Gap Energy: Experimental Results vs DFT-Based Calculations

Muhammad Dipa Pramudita Budiyana[1], Muhammad Ziddan Rachman[1], *Pina Pitriana[1], & Diah Mulhayatiah[1]
[1]Physics Education Study Program, UIN Sunan Gunung Djati Bandung, Indonesia
*Corresponding Author: pinapitriana@uinsgd.ac.id

Received: 25th September 2025; **Accepted**: 16th March 2026; **Published**: 23rd April 2026
DOI: https://dx.doi.org/10.29303/jpft.v12i1.10241

Abstract - *This study aims to analyze the density of states (DOS) of boron arsenide (BAs) using two types of pseudopotentials, namely PBE ultrasoft and PBE-PAW, within the framework of density functional theory (DFT). The resulting DOS profiles show that both methods are able to capture the fundamental electronic characteristics of the material, with similar energy distribution patterns, although differences are observed in the detailed features of the curves. The PBE-PAW method produces smoother and more representative results near the atomic nucleus, whereas the PBE ultrasoft approach exhibits sharper and more fluctuating peaks. Around the Fermi energy level, the density of states approaches zero, indicating the semiconducting nature of the material. The estimated band gap is in the range of 1.5–2.5 eV, suggesting that BAs has potential applications in electronic devices, sensors, and photovoltaic technologies. Based on these findings, further studies are recommended to validate the band gap using hybrid functionals or the GW approximation, to investigate phonon behavior and thermal conductivity, and to optimize pseudopotential selection for high-precision electronic property calculations in future device-oriented applications.*

Keywords*: Band gap; Boron Arsenide (BAs); Density Functional Theory (DFT); Density of States (DOS); Pseudopotensial (PBE-Ultrasoft, PBE-PAW)*

INTRODUCTION

Boron arsenide (BAs) is an interesting semiconductor material due to its exceptional thermal properties, namely the ability to conduct heat efficiently with a thermal conductivity value of approximately 1300 W/mK. With this property, boron arsenide can be used as an excellent heat management material, helping to prevent overheating in modern electronic and photonic devices (Mandel, 2019).

This material also possesses optical and mechanical properties that have been experimentally measured, including the optical refractive index, elastic modulus, and thermal expansion coefficient. The main advantage of boron arsenide compared to traditional semiconductor materials such as silicon is its ability to manage heat efficiently, which is crucial for improving the performance and sustainability of increasingly smaller and more complex electronic devices (Mandel, 2019).

High thermal conductivity materials are essential to ensure effective heat management and maintain device performance (Hou et al., 2024). However, carbon-based materials such as diamond and graphite have limitations, including high cost, environmental sensitivity, and anisotropic properties, thereby creating a need for more efficient alternatives (Kang et al., 2018).

In this context, Boron Arsenide (BAs) itself is a III–V group semiconductor compound that has attracted attention due to its potential as a superior thermal material. Cubic Boron Arsenide (c-BAs) is predicted to have thermal conductivity exceeding 2000 W/m·K at room temperature and up to 3000 W/m·K under isotopically pure conditions, approaching the performance of diamond at a lower cost (Zhong et al., 2025).

Furthermore, its compatibility with semiconductor materials such as silicon (Si), gallium nitride (GaN), and gallium arsenide (GaAs) makes it ideal for modern electronic applications.

Its stable crystal structure and narrow bandgap (~1.8 eV) open opportunities for use in various optoelectronic and thermal applications. Nevertheless, the synthesis process of BAs still faces significant challenges, such as the instability of boron and arsenic composition during epitaxy and cooling processes, as well as limitations in producing defect-free single crystals (Hou et al., 2024).

Technological advances have enabled the production of defect-free crystals suitable for thermal conductivity measurements, but traditional measurement methods such as time-domain thermoreflectance (TDTR) often require a metal layer as a thermal transducer, which increases measurement complexity. To overcome these limitations, the nanosecond, transducer-less time-domain thermoreflectance (tl-TDTR) method has been developed to allow faster and more accurate measurements. Using this method, c-BAs has been proven to have ultra-high thermal conductivity (>2000 W/m·K), even exceeding the previously theoretical limit of around 1300 W/m·K. The thermal conductivity of BAs also strongly depends on crystal quality. Crystals with stronger photoluminescence (PL) intensity and longer PL lifetimes exhibit higher thermal conductivity, although measured PL lifetimes are still shorter than expected (Zhong et al., 2025).

This finding also challenges existing theoretical models, including Slack's rule, which has been a reference for determining materials with high thermal conductivity. Recent studies show that unique features in BAs phonon dispersion, such as the large gap between acoustic and optical phonon frequencies, can reduce phonon scattering and enhance thermal transport efficiency. With this great potential, Boron Arsenide (BAs) offers a promising solution to improve thermal efficiency and future electronic device performance, while also encouraging further research to understand the microscopic mechanisms underlying the material's performance (Zhong et al., 2025).

In addition to its thermal advantages, the electronic aspects of Boron Arsenide, particularly the band gap energy, are crucial parameters that determine its semiconductor characteristics. The band gap value affects the material's optoelectronic response and determines its ability to transmit or absorb light within specific energy ranges (Buckeridge & Scanlon, 2019). Therefore, accurately knowing the band gap energy is essential for designing applications such as infrared detectors, solar cells, and other photonic devices (Acharya et al., 2024). However, reported band gap values in the literature still show variations, depending on the computational approach used, whether through empirical theoretical models or first-principles simulation methods such as Density Functional Theory (DFT) (Buckeridge & Scanlon, 2019).

The Density Functional Theory (DFT) method has become a highly reliable tool for predicting the electronic properties of materials, including energy band structures and band gaps. Nevertheless, standard DFT often faces limitations in accurately estimating the band gap due to the approximations in the exchange-correlation functional used. Therefore, it is important to conduct a comparative study between experimental results and DFT simulation outcomes in the context of Boron Arsenide to gain a more comprehensive understanding of the material's electronic properties and to identify potential deviations or

inconsistencies between theory and simulation results (Acharya et al., 2024).

Based on the background above, several research questions are formulated:

1. How do the crystal structure and atomic configuration of Boron Arsenide (BAs) affect its electronic and thermal properties?
2. How accurate is the Density Functional Theory (DFT)-based computational method in predicting the electronic properties of BAs, particularly its band gap and total energy?
3. What is the effect of simulation parameter variations, such as pseudopotential type and K-point values, on SCF and DOS calculation results for the BAs compound?

RESEARCH METHODS

In this study, the computational method used was Density Functional Theory (DFT). DFT is a computational approach that simplifies the solution of the Schrödinger equation by relying on the electron density. Electron-electron interactions are aggregated within the density, which requires an initial guess in terms of the potential (pseudopotential). The calculations were performed using the Burai 1.3 Graphic User Interface (GUI) of the Quantum ESPRESSO program (Tyagi & Negi, 2023).

Before performing the calculations, the first step was to determine the crystal structure of the Boron Arsenide (BAs) compound using BURAI software. To visualize the material's structure, input data in the form of lattice constants and atomic configuration elements were obtained from the AFLOW Automatic Flow of Materials Discovery database. The structure file was downloaded in CIF (Crystallographic Information File) format and then imported into BURAI for further processing.

After the structure was visualized, the next step involved calculations using the Self-Consistent Field (SCF) method to obtain the system's total energy. These calculations were performed by varying the K-point grid values at (2×2×2), (4×4×4), (6×6×6), (8×8×8), and (10×10×10), as well as selecting the appropriate pseudopotential type, namely ultrasoft-PBE and PAW-PBE, both of which are optimal for simulating semiconductor systems such as BAs.

It should be noted that in this study, K-points were applied in two distinct calculation stages, namely SCF and Density of States (DOS) calculations. For SCF calculations, K-point variations were used to determine the parameters that yield the most stable total energy, which were then plotted against each K-point as shown in Figure 1. This plot helps identify the most optimal configuration for subsequent calculations.

Table 1. Parameter Variations

No.	K-Points on SCF	K-Points on DOS	Pseudopotential
1	4 × 4 × 4	8 × 8 × 8	PBE-Ultrasoft
2			PBE-PAW
3	6 × 6 × 6	10 × 10 × 10	PBE-Ultrasoft
4			PBE-PAW
5	8 × 8 × 8	12 × 12 × 12	PBE-Ultrasoft
6			PBE-PAW
7	12 × 12 × 12	14 × 14 × 14	PBE-Ultrasoft
8			PBE-PAW
9	14 × 14 × 14	16 × 16 × 16	PBE-Ultrasoft
10			PBE-PAW

Meanwhile, in the DOS calculation stage, the K-points used must be denser or higher than those used in SCF. This is because DOS calculations require higher energy resolution to accurately depict the distribution of electronic energy levels. A denser K-point grid allows for a more detailed representation of the energy spectrum, so that DOS calculations can

precisely reflect the density of electronic states.

The K-point variations used in SCF calculations serve as a basis for further analysis regarding the effect of sampling point density in the Brillouin zone on simulation accuracy. This is explained in the following section, which discusses in detail the correlation between K-point configurations and the representation of electronic distribution in the Boron Arsenide crystal structure.

In this study, variations in K-point grids and pseudopotentials were applied to obtain the lowest total energy through SCF calculations using BURAI software. These parameter variations are crucial to ensure that the simulation results are convergent and accurate.

K-points are closely related to the representation of the Brillouin zone, which is the space used in calculating the electronic properties of crystalline materials. K-points are sampling points in reciprocal space that help solve the distribution of electrons within the crystal. The denser the K-point grid (e.g., from 2×2×2 to 10×10×10), the more precise the Brillouin zone representation, as more sampling points capture electron distribution between atoms. This is important because it can affect the accuracy of total energy calculations, especially in semiconductor systems such as Boron Arsenide.

Table 2. Crystal Structure and Atomic Coordinates

BAs [Cubic FCC]										
Fractional Coordinates				**Latic Parameters**						
				(angstrom)				(°)		
Atom	x	y	z	a	b	c	c/a			
B	0.25	0.25	0.25	3.40	3.40	3.40	1	60	60	60
As	0	0	0							

RESULTS AND DISCUSSION

The experiments conducted during the SCF process produced observational data for the lowest total energy of the BAs compound based on variations in K-point parameters and pseudopotentials in SCF calculations, as shown in Table 3.

Table 3. Total Energy of BAs Compound Based on K-Point and Pseudopotential Variations

No.	**K-Points**	**Pseudopotential**	**Total Energy (Ry)**
1	6 × 6 × 6	PBE-Ultrasoft	-106.53983054
2		PBE-PAW	-749.81213936
3	8 × 8 × 8	PBE-Ultrasoft	-106.5398536
4		PBE-PAW	-749.81217907
5	10 × 10 × 10	PBE-Ultrasoft	-106.53985011
6		PBE-PAW	-749.8121813
7	12 × 12 × 12	PBE-Ultrasoft	-106.53986094
8		PBE-PAW	-749.81218172
9	14 × 14 × 14	PBE-Ultrasoft	-106.53986026
10		PBE-PAW	-749.81218111

Based on Table 3, variations in K-point parameters and pseudopotentials used for BAs result in different total energies. For example, comparing experiment 1 with experiment 3, experiment 1 with a K-point of 6 × 6 × 6 yielded a total energy of -106.53983054 Ry, while experiment 3 with a K-point of 8 × 8 × 8 produced -106.5398536 Ry. This indicates that the K-point affects the total energy of the BAs compound.

Furthermore, the choice of

pseudopotential also influences the total energy. For instance, experiments 1 and 2 used the same K-point but different pseudopotentials, resulting in different total energies. Experiment 1 with PBE-Ultrasoft yielded -106.53983054 Ry, whereas experiment 2 with PBE-PAW yielded -749.81213936 Ry. The relationship between K-points and total energy for BAs can be observed in Figure 1.

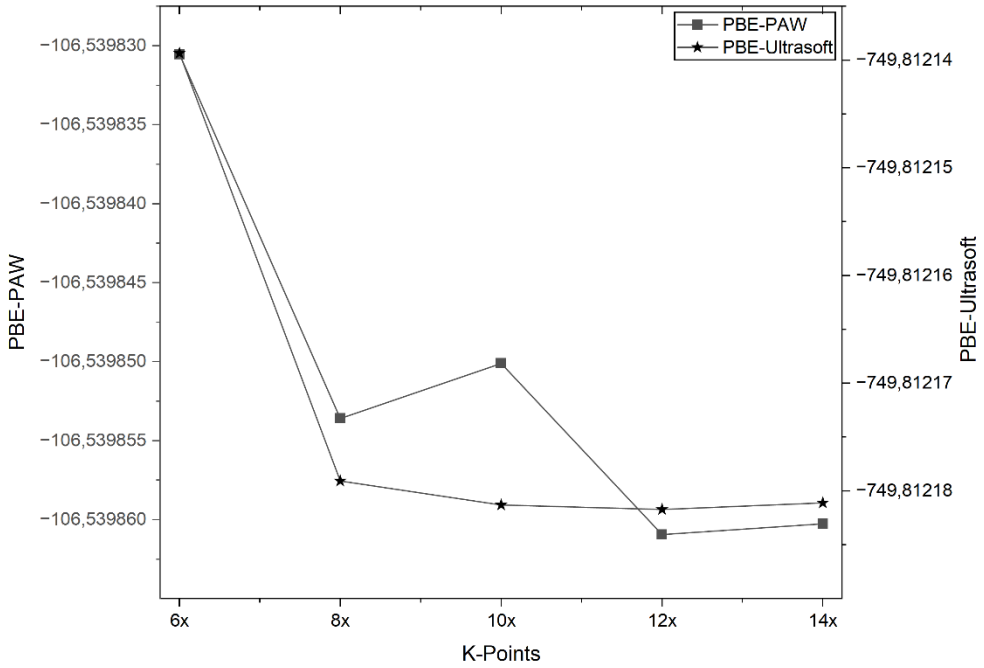

Figure 1. Relationship between K-Points and Total Energy of BAs Using PBE-Ultrasoft and PBE-PAW Pseudopotentials

In Figure 1, the black line represents total energy distribution for BAs using PBE-Ultrasoft pseudopotential, while the red line represents PBE-PAW. Both pseudopotentials show that total energy stabilizes at K-points 12 × 12 × 12, with values of -106.53986094 Ry (PBE-Ultrasoft) and -749.81218172 Ry (PBE-PAW). The K-point variation shows a trend of increasingly stable total energy convergence on the 12×12×12 grid. This indicates that the Brillouin zone sampling at this density is sufficient to represent the electron distribution in the BAs crystal. This convergence is important because it determines the accuracy of the band structure and DOS in the next stage.

The PBE-PAW pseudopotential provides a more stable total energy than PBE-Ultrasoft, meaning the PAW method is able to reconstruct the wave function in the nuclear region more accurately. This results in a more representative description of the electron–nuclear interaction, especially for light atoms such as boron and arsenic. Meanwhile, PBE-Ultrasoft tends to produce small fluctuations in the charge density, which is reflected through sharper and less smooth DOS peaks. This difference in characteristics explains why the PBE-PAW DOS curve appears smoother and more physical. Additionally, the SCF output provides Fermi energy for both pseudopotentials at each K-point, as summarized in Table 4.

Table 4. Fermi Energy of BAs

No.	K-Points	Fermi Energy (eV)	
		PBE-Ultrasoft	PBE-PAW
1	6 × 6 × 6	8,9271	8,9156
2	8 × 8 × 8	8,8588	8,9247
3	10 × 10 × 10	8,9337	8,9261
4	12 × 12 × 12	8,9530	8,9386
5	14 × 14 × 14	8,9460	8,9290

With the Fermi energies obtained from each experiment, the band structure for each variation was calculated to determine the energy gap between the valence and conduction bands of BAs.

The band gap for BAs with the PBE-PAW pseudopotential is shown in Figure 2, while PBE-Ultrasoft results are shown in Figure 3. The Fermi energy represents the boundary between the valence and conduction bands and serves as the highest energy level in the valence band.

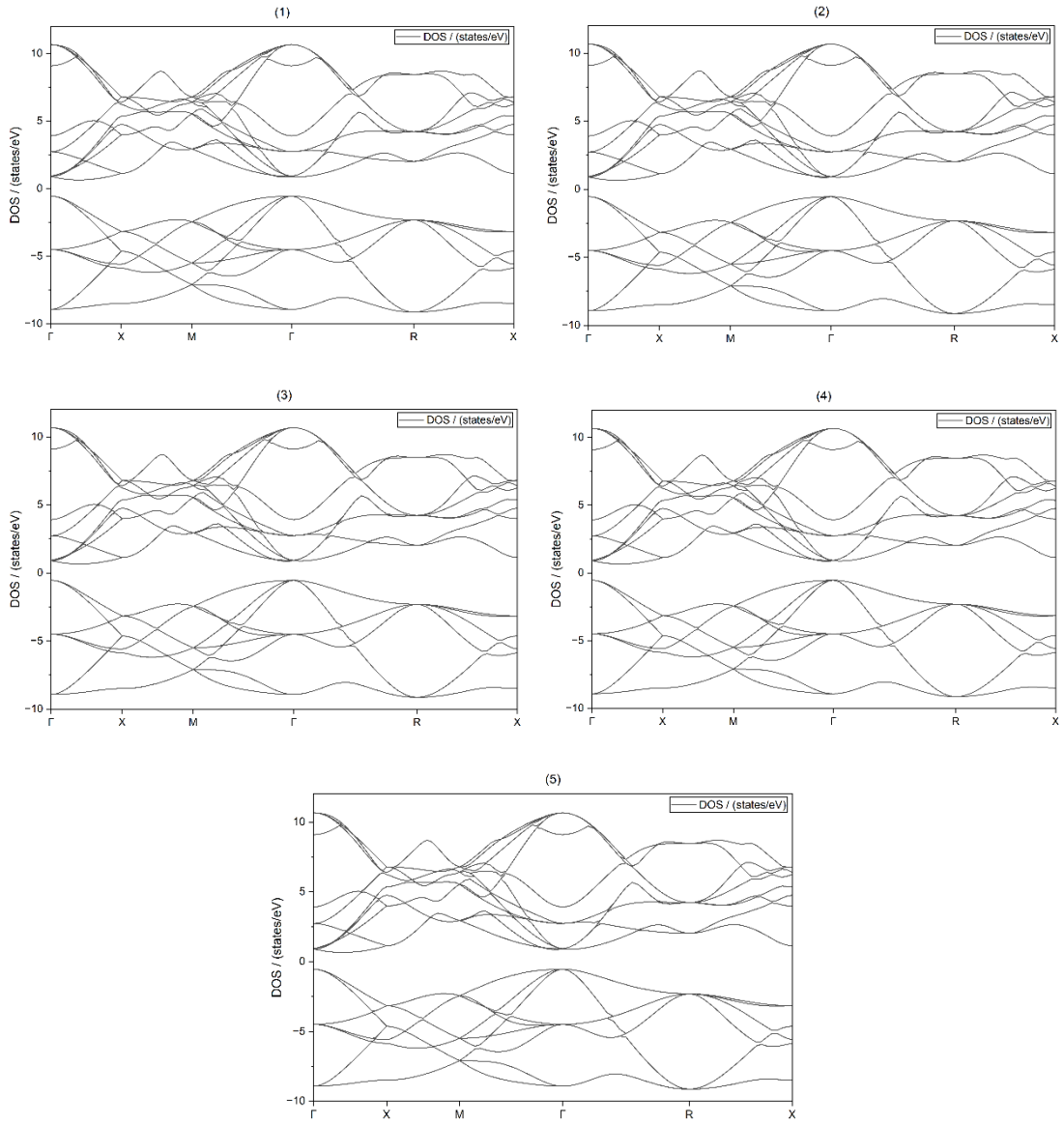

Figure 2. Band Gap of BAs with PBE-PAW; (1) 6 × 6 × 6 (2) 8 × 8 × 8 (3) 10 × 10 × 10 (4) 12 × 12 × 12 (5) 14 × 14 × 14

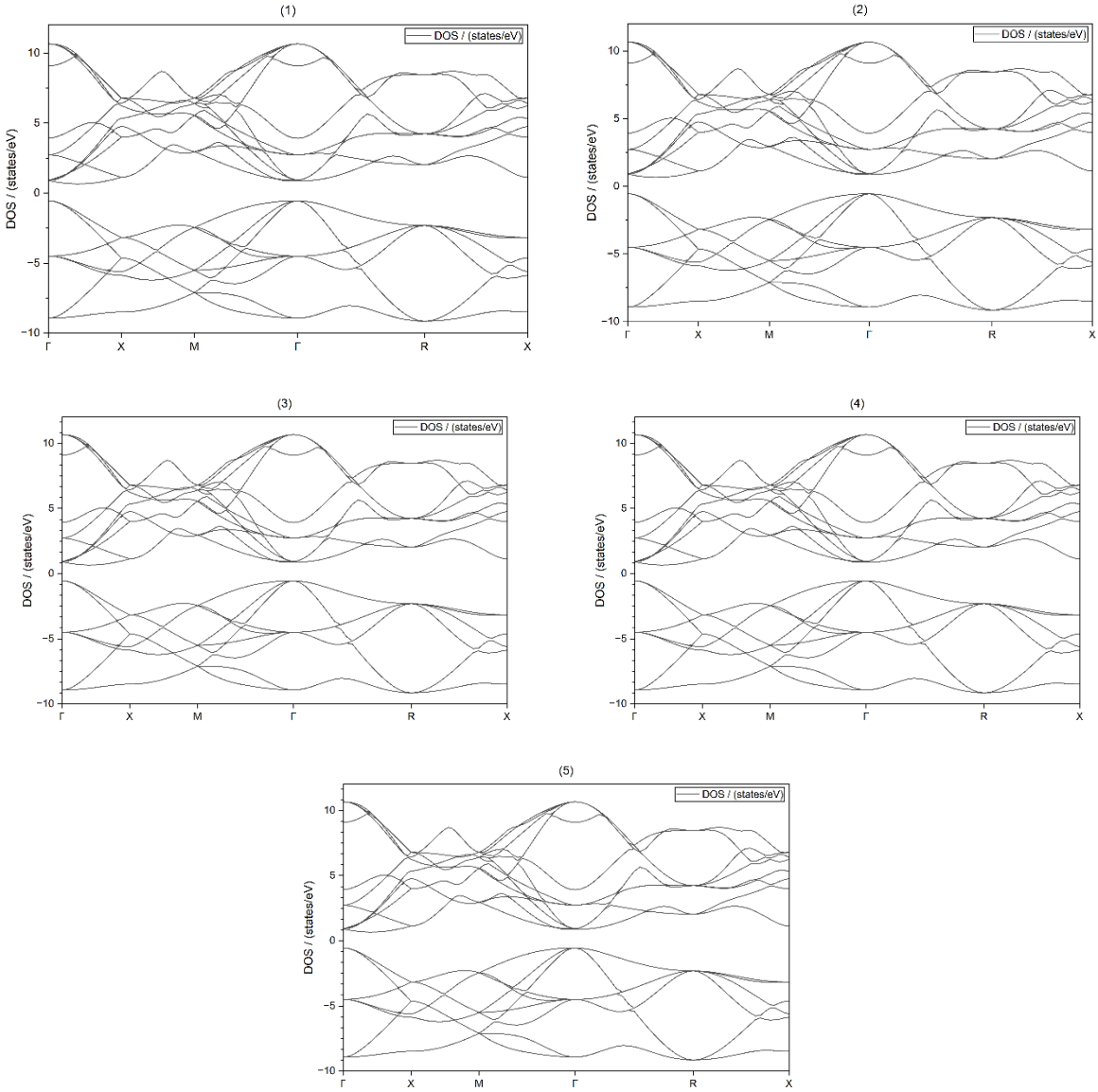

Figure 3. Band Gap of BAs with PBE-Ultrasoft; (1) 6 × 6 × 6 (2) 8 × 8 × 8 (3) 10 × 10 × 10 (4) 12 × 12 × 12 (5) 14 × 14 × 14

From Figures 2 and 3, the band gap is obtained by subtracting the minimum conduction band energy from the maximum valence band energy. In this representation, the valence band is shown from zero downwards (negative Y-axis), and the conduction band is shown from zero upwards (positive Y-axis). In other words, the conduction band corresponds to the lowest energy, while the valence band corresponds to the maximum energy. The band gaps for ten experiments varying K-points and pseudopotentials are shown in Table 5.

Table 5. Band Gap of BAs

Conduction Bands (eV)		Valence Bands (eV)		Energi Gap (eV)	
PBE-Ultrasoft	**PBE-PAW**	**PBE-Ultrasoft**	**PBE-PAW**	**PBE-Ultrasoft**	**PBE-PAW**
0.5904	0.5860	-0.6149	-0.6085	1.2053	1.1945

Conduction Bands (eV)		Valence Bands (eV)		Energi Gap (eV)	
PBE-Ultrasoft	**PBE-PAW**	**PBE-Ultrasoft**	**PBE-PAW**	**PBE-Ultrasoft**	**PBE-PAW**
0.6586	0.5769	-0.5467	-0.6176	1.2053	1.1945
0.5837	0.5755	-0.6216	-0.6190	1.2053	1.1945
0.5644	0.5630	-0.6409	-0.6315	1.2053	1.1945
0.5714	0.5726	-0.6339	-0.6219	1.2053	1.1945

Based on Table 5, each K-point produces the same band gap, 1.20 eV for PBE-Ultrasoft and 1.19 eV for PBE-PAW, indicating that K-points do not significantly affect the band gap in this calculation. According to Kang et al. (2019), experimental measurements using UV–Vis absorption spectroscopy reported a BAs band gap of 1.82 eV, while computational results from Duke University yielded 1.2 eV (Materials Page - As1B1.

The calculated band gap using BURAI 1.3.2, a GUI of Quantum ESPRESSO, was compared with previous experimental results to determine the error. The comparison of BAs band gaps is shown in Table 6.

Table 6. Comparison of BAs Band Gap from Computation and Reference

Pseudopotential	Gap Energy (eV)			Error (%)	
	Computation	Reference			
		Computation	Experiment	Computation	Experiment
PBE-Ultrasoft	1.20	1.20	1.82	0.27	33.77
PBE-PAW	1.19	1.20	1.82	0.62	34.37

Table 6 shows that the lowest error is obtained using PBE-Ultrasoft, 0.27%. The simulated band gap (1.19–1.20 eV) is lower than the experimental value (1.82 eV). This occurs because the use of generalized gradient approximation (GGA-PBE) systematically reduces (underestimates) the energy gap due to the inaccurate representation of electron-electron correlations. More sophisticated methods such as HSE06, PBE0, or GW can correct this deficiency by incorporating self-energy effects, thus usually producing band gaps that are closer to the experimental value. This highlights a significant discrepancy between computational and experimental values.

The DOS results for PBE-Ultrasoft and PBE-PAW pseudopotentials are shown in Figures 4 and 5.

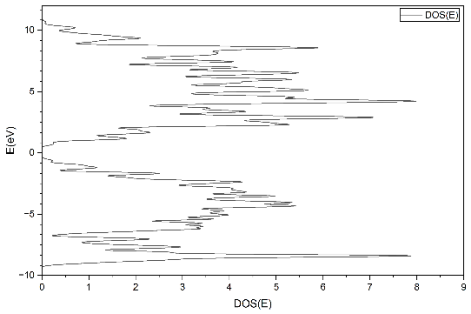

Figure 4. DOS for PBE-Ultrasoft

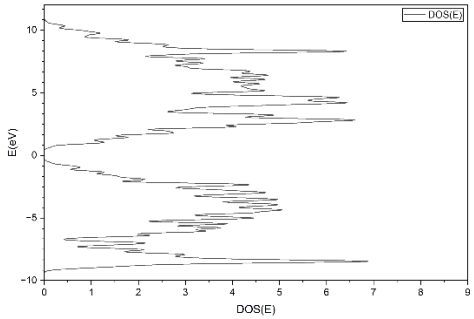

Figure 5. DOS for PBE-PAW

The horizontal axis represents energy in electronvolts (eV), and the vertical axis represents the number of quantum states per unit energy (DOS, states/eV). Both graphs

span the same energy range, from -17.5 eV to 12.5 eV, with zero energy set at the Fermi level (highest occupied energy at 0 K).

Overall, DOS patterns are very similar for both PBE-Ultrasoft and PBE-PAW, indicating that both methods capture the same fundamental electronic structure. However, differences exist in detail and smoothness. PBE-PAW produces smoother curves, reflecting its ability to represent near-core states more accurately, while ultrasoft produces sharper, more fluctuating peaks.

Below -10 eV, sharp peaks correspond to core-like states, such as 2s/2p orbitals of light elements or d orbitals of transition metals. The most striking phenomenon occurs around the Fermi level (energy = 0 eV). In both graphs, the density of states drops sharply to zero, with no peak or continuation from the valence band to the conduction band. This is a characteristic feature of semiconductors or insulators, as no quantum state can be occupied exactly at the Fermi energy.

Therefore, to make these systems conduct electricity, it is necessary to excite electrons from the valence band to the conduction band,

across the band gap. Above the Fermi level, from 0 to +10 eV, there are a large number of dense and graded DOS peaks,

indicating the presence of a complex conduction band.

The curves in the PBE-Ultrasoft curve show sharp fluctuations, while the PBE-PAW curves exhibit smoother fluctuations, but retain similar band topological characteristics. This shows that both methods consistently capture key electronic features, although the details differ due to the different representations of wave functions near the nucleus.

The final interpretation of the two graphs indicates that the analyzed material is likely a semiconductor with a band gap of around 1.5 to 2.5 eV, based on visual observation of the positions of the last energy point of the valence band and the beginning of the conduction band. Such a material could be suitable for photovoltaic applications, sensors, or other electronic devices, depending on the structure and characteristics of the orbitals that dominate the valence and conduction bands. A band gap that is neither too large nor too small indicates that the material has the potential for high efficiency in energy conversion or charge transport.

CONCLUSION

This study demonstrates that Boron Arsenide (BAs) has significant potential as a high-performance semiconductor and thermal material. Through DFT-based simulations with variations in pseudopotentials and K-points, crucial information regarding total energy stability, Fermi energy, as well as band structure and density of states (DOS) was obtained. The most stable total energy was achieved at a K-point of 12×12×12, while the band gap obtained from simulations ranged from 1.19 to 1.20 eV. Although these values are slightly lower than experimental results (~1.82 eV), such discrepancies are common in conventional DFT approaches.

Both pseudopotentials (PBE-Ultrasoft and PBE-PAW) effectively represent the electronic properties of the material, with PBE-PAW providing smoother and more realistic results, particularly in the valence and conduction band regions. The semiconductor characteristics of BAs are clearly indicated by the presence of a gap at the Fermi level, and the band structure shows a consistent energy gap. With its exceptionally high thermal conductivity and good electronic compatibility, BAs holds great potential for future electronic and

optoelectronic devices, such as sensors, microelectronic coolers, and solar cells. Further research is recommended to explore more accurate computational methods for predicting the band gap, as well as high-quality material synthesis techniques.

REFERENCES

Acharya, S., Pashov, D., Katsnelson, M. I., & van Schilfgaarde, M. (2024). One-Particle and Excitonic Band Structure in Cubic Boron Arsenide. *Physica Status Solidi (RRL) – Rapid Research Letters*, *18*(1). https://doi.org/10.1002/pssr.202300156

Buckeridge, J., & Scanlon, D. O. (2019). Electronic band structure and optical properties of boron arsenide. *Physical Review Materials*, *3*(5), 051601. https://doi.org/10.1103/PhysRevMaterials.3.051601

Hou, S., Pan, F., Shi, X., Ebrahim Nataj, Z., Kargar, F., Balandin, A. A., Cahill, D. G., Li, C., Ren, Z., & Wilson, R. B. (2024). Ultrahigh thermal conductivity of cubic boron arsenide with an unexpectedly strong temperature dependence. *ArXiv E-Prints*, arXiv-2402.

Kang, J. S., Li, M., Wu, H., Nguyen, H., & Hu, Y. (2018). Experimental observation of high thermal conductivity in boron arsenide. *Science*, *361*(6402), 575–578. https://doi.org/10.1126/science.aat5522

Mandel, S. (2019). Properties of boron arsenide – a semiconductor with ultrahigh thermal conductivity. *Scilight*, *2019*(38). https://doi.org/10.1063/10.0000023

Tyagi, S., & Negi, S. (2023). Calculation of density of states of pristine and functionalized carbon nanotubes: A dft approach. *Indian Journal of Science and Technology*, *16*(40), 3567–3574.

Zhong, H., Peng, Y., Lin, F., Niyikiza, A. B., Pan, F., Qin, C., Chen, J., Hadjiev, V. G., Deng, L., & Ren, Z. (2025). Thermal Conductivity above 2,000 W/m· K in Boron Arsenide by Nanosecond Transducer-Less Time-Domain Thermoreflectance. *Research*, *8*, 0971.